N73-18448

NASA TECHNICAL REPORT

NASA TR R-404

NASA TR R-404

CASE FILE COPY

THE TECHNIQUES OF HOLOGRAPHIC PARTICLE SIZING

by Robert L. Kurtz

George C. Marshall Space Flight Center
Marshall Space Flight Center, Ala. 35812

NATIONAL AERONAUTICS AND SPACE ADMINISTRATION • WASHINGTON, D. C. • MARCH 1973

TECHNICAL REPORT STANDARD TITLE PAGE

1. REPORT NO.	2. GOVERNMENT ACCESSION NO.	3. RECIPIENT'S CATALOG NO.
TR R-404		

4. TITLE AND SUBTITLE	5. REPORT DATE
The Techniques of Holographic Particle Sizing	March 1973
	6. PERFORMING ORGANIZATION CODE
7. AUTHOR(S)	8. PERFORMING ORGANIZATION REPORT #
Robert L. Kurtz	M454
9. PERFORMING ORGANIZATION NAME AND ADDRESS	10. WORK UNIT NO.
George C. Marshall Space Flight Center Marshall Space Flight Center, Alabama 35812	11. CONTRACT OR GRANT NO.
	13. TYPE OF REPORT & PERIOD COVERED
12. SPONSORING AGENCY NAME AND ADDRESS	Technical Report
National Aeronautics and Space Administration Washington, D.C. 20546	14. SPONSORING AGENCY CODE

15. SUPPLEMENTARY NOTES

Prepared by Space Sciences Laboratory, Science and Engineering

16. ABSTRACT

Depending on the mechanism of particle production, the resultant particle size and velocity distribution may range over several orders of magnitude. In general, if particle size information is desired from a given type generator, one must resort to some form of experimental determination of the distribution. If the source of particle production is a dynamic one involving a reasonable volume, holography provides a tailor-made particle size and velocity distribution detector. This is evidenced by the fact that holography allows the entire volume to be recorded on one exposure without any interference with the volume of interest. Herein lies a very important characteristic of the holographic particle detection technique: It provides a holographic nondestructive testing technique in the fullest sense of the definition of nondestructive testing. This report provides a description of three different systems useful in this technique and includes the experimental results from one of the holographic systems which was used to detect particle size and velocity distribution from the Skylab waste tank.

17. KEY WORDS	18. DISTRIBUTION STATEMENT

19. SECURITY CLASSIF. (of this report)	20. SECURITY CLASSIF. (of this page)	21. NO. OF PAGES	22. PRICE
Unclassified	Unclassified	21	$3.00

For sale by National Technical Information Service, Springfield, Virginia 22151

TABLE OF CONTENTS

LIST OF ILLUSTRATIONS

THE TECHNIQUES OF HOLOGRAPHIC PARTICLE SIZING

INTRODUCTION

Depending on the mechanism of particle production, the resultant particle size distribution may range over several orders of magnitude. In general, if particle size information is desired from a given type generator, one must resort to some form of experimental determination of these distributions. The generators of such particles of interest may be anything from smoke stacks which produce common air pollutants to the Skylab waste tank which produces possible contaminants of scientific experiments in earth orbit.

If the source of particle production is dynamic and involves a reasonable volume, holography provides a tailor-made particle size and velocity distribution detector. This is evidenced by the fact that holography allows the entire volume to be recorded on one exposure, and, consequently, one may inspect the recorded volume for particle size and velocity distribution at some later, more convenient time. Further, the desired distribution is obtained from the dynamic (or static) volume while leaving this volume totally undisturbed.

Herein lies a very important characteristic of the holographic particle detection technique. It provides a holographic nondestructive testing (HNDT) technique in the fullest sense of the definition of nondestructive testing. Even though when one normally says holographic nondestruct testing, one thinks of an interferometric fringe technique, it is suggested that the holographic particle sizing technique now be included as a new nondestructive method of evaluation, since that is precisely what it accomplishes. Further, the actual evaluation of the data from this technique is much more thoroughly understood and straightforward than is the evaluation of the fringe analysis demanded by the usual form of HNDT.

To obtain velocity information with this technique, one may simply double pulse the hologram field with a known time delay between the pulses. By measuring the distance vector between the two images of a given particle, one may obtain the velocity for that particle. Experimental results for this type of testing have been obtained and will be presented later in this report.

A theoretical analysis of the in-line holographic recording system is presented along with a description of two possible holographic particle detection techniques: the in-line and acute-sideband techniques. Both of these systems may be thought of as imaging systems which measure particles down to 10 μm in diameter. Another technique, called submicron particle detection, which allows the detection of particles down to 0.1 μm in diameter will be briefly discussed.

Finally, a large and very useful bibliography has been included which lists some of the more important publications available on this subject. Any worker just entering this field will find this invaluable.

THEORETICAL ANALYSIS OF RECORDING SYSTEM

The film records the interference pattern between two wavefronts from the object plane of the sample volume. One wavefront which is undiffracted constitutes the reference wavefront; the other is caused by the radiation diffracted by the particles and is called the object wavefront. These wavefronts add coherently in the film plane to produce the

field given by

$$E(\bar{z}) = E_1 e^{i\phi_1} + E_2 e^{i\phi_2} \qquad (1)$$

where E_1 and E_2 are the amplitudes of the reference and object beams, respectively, and ϕ_1 and ϕ_2 are their respective phases. The film records only intensity given by

$$I = \left|E(\bar{z})\right|^2 = E_1{}^2 + E_2{}^2 + E_1 E_2 \left[e^{i(\phi_1 - \phi_2)} + e^{-i(\phi_1 - \phi_2)} \right] \quad . \qquad (2)$$

The developed negative has amplitude transmittance given by

$$T(z) \alpha (It)^{-\gamma/2} \qquad (3)$$

where γ is the slope of the linear portion of the Heurter Driffield (D-log E) curve for the film, and t is the exposure time for the film. If one substitutes equation (2) for the intensity, it is found that the amplitude transmittance of the hologram is

$$T(z) \alpha \left\{ \left[E_1{}^2 + E_2{}^2 + 2E_1 E_2 \cos(\phi_1 - \phi_2) \right] t \right\}^{-\gamma/2} . \qquad (4)$$

If one assumes sufficient amplitude for the reference beam, it is possible to binomially expand equation (4) and drop higher order terms to get

$$T(z) = k \left\{ E_1{}^2 - \frac{\gamma}{2} E_2{}^2 - \frac{\gamma}{2} \left[E_1 E_2 e^{i(\phi_1 - \phi_2)} + e^{-i(\phi_1 - \phi_2)} \right] \right\} \qquad (5)$$

where k is a constant and equal to $E^{-(\gamma + 2)} t^{-\gamma/2}$. On reconstruction of the hologram, the incident radiation is attenuated and diffracted according to this equation. The attenuation is provided by the first two terms. The first term represents a constant attenuation of the incident beam; the second term attenuates according to the recorded amplitude variation of the diffracted wave and is affected by the developed γ for the film. The third and fourth terms contain the information necessary to reconstruct the real and virtual images of the particle field, respectively.

If one desires to discuss the reconstruction process, it is noted that these terms diffract and attenuate radiation passing through the hologram in such a way that concave and convex wavefronts emerge from the hologram which, when traced to the Fraunhofer region, allow the two images to separate. To understand how these wavefronts are formed in a Fraunhofer hologram, it is necessary to look at the derivation of the Fraunhofer diffraction pattern of an opaque particle. Belz uses an approach similar to the above and shows that the intensity in the observation plane is

$$I = 1 - \frac{2k}{z} \sin\left(\frac{k|\bar{\rho}|^2}{2z}\right) \left[\widetilde{D}(\bar{\rho})\right] \frac{k^2}{z^2} \left[\widetilde{D}(\bar{\rho})\right]^2 \qquad (6)$$

where

$$\widetilde{D}(\bar{\rho}) = \int D(\bar{\xi}) \exp\left[- \frac{ik(\bar{\xi} - \bar{\rho})}{z} \right] d\bar{\xi} \qquad (7)$$

is the Fourier transform of the particle in the object plane.

Therefore, since the theoretical development for the reconstruction is well documented (Belz, and Trolinger, et al.), it will not be further reproduced here.

SYSTEM DESCRIPTION

In-Line System

This is the system used most extensively to date. It is patterned after the original system offered by Dr. Dennis Gabor in 1948; for this reason it is sometimes referred to as the Gabor system. However, unlike the Gabor system, which performs its detection in the Fresnel region, the in-line system places the film detector in the Fraunhofer region. The film may still be in the Fresnel region of the total ensemble of target particles, yet it must be in the far field, or Fraunhofer region, of each individual particle. Because of this, the double-image problem which plagued Gabor is avoided. The specific definition of Fresnel and Fraunhofer regions will be given in the next section.

The in-line system may be described in general by the illustration in Figure 1. A plane wavefront beam is incident on and passes through some target volume of interest. The presence of individual particles distributed throughout this volume essentially causes the plane wave to become scattered and diffracted at many points so as to produce a spherical wave as well as a plane wave. The plane wave is, of course, that part of the incident wave which passes through the target field region undisturbed. The undisturbed plane wave then constitutes the holographic reference beam. The spherical wave produced by the diffraction around the individual particles constitutes the holographic object beam. These two waves interfere at the film plane and the interference pattern so recorded at the film plane provides the means for reconstructing the real image of the target field region. This real image may be inspected and analyzed at a later time to provide quantitative information about the individual particles making up the target field. The distance z between target particle and film plane is determined from the Fraunhofer condition for that individual particle. The specific details of this are covered in the previous and succeeding sections. It is the purpose of this section to provide a general and more intuitive description of the holographic system.

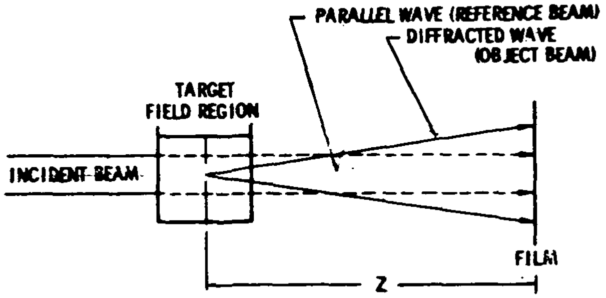

Figure 1. Gabor in-line system.

To provide a further intuitive breakdown of the in-line system, attention is directed to Figure 2. Here all things are as in Figure 1, except that one considers only three individual particles of the field and the diffraction which occurs at these particles to produce the necessary spherical wavefronts to be used as object beam in producing the interference at the film plane. Again, most of the incident plane waves must pass through undisturbed in order to provide a sufficient reference wave. One point which must be mentioned here is that the incident wave need not be a plane or parallel wave, but most of the incident beam must pass through undisturbed if one is to have a sufficient reference wave. A parallel, i.e., plane, incident wave does provide a distinct advantage, however, in that it provides unity magnification throughout the field volume.

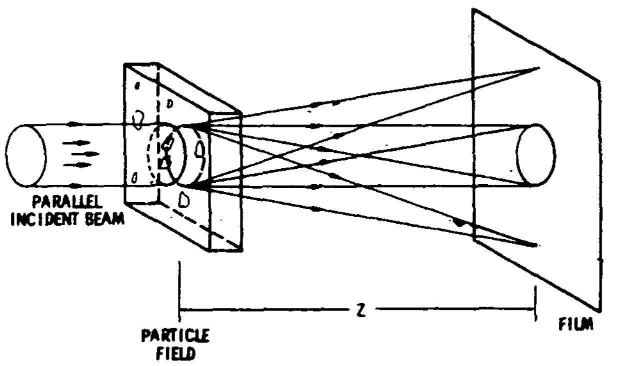

Figure 2. Particle field diffraction.

To further illucidate the physics of what happens at each particle in the field volume, attention is directed to Figure 3 where only a single particle of the entire field volume is considered. Consider what happens physically from a nonmathematical, zone-plate analysis.

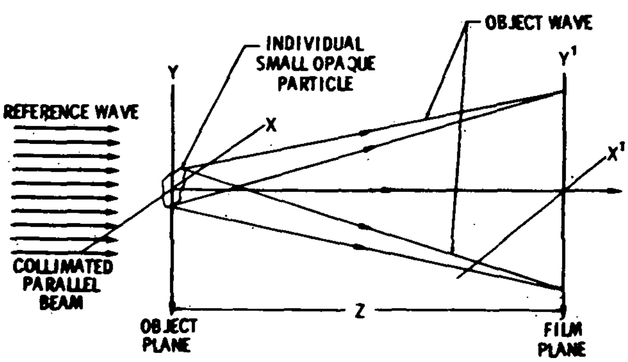

Figure 3. Single particle diffraction.

Consider a rather simple interference pattern between a set of plane waves (reference wave) and a set of spherical waves (object wave) caused by diffraction around the single opaque particle of Figure 3. When these two waves meet in phase at the film plane, they reinforce each other, their energy adds and, accordingly, the plate is more strongly exposed there. At the point in the film plane where the waves meet out of phase by 180 deg, they essentially cancel each other, assuming equal amplitude. At this point the film is very weakly exposed or not exposed at all. Points in the film plane, (x', y'), having some intermediate phase between 0 and 180 deg respond accordingly. The total interference between these two sets of waves causes a holographic zone plate to be recorded. The holographic zone plate of course varies sinusoidally and does not have the square-wave response of a manufactured zone plate. Yet, to first order they may be considered the same. The total arrested interference pattern caused by the set of waves in Figure 3 will then look like the zone plate of Figure 4.

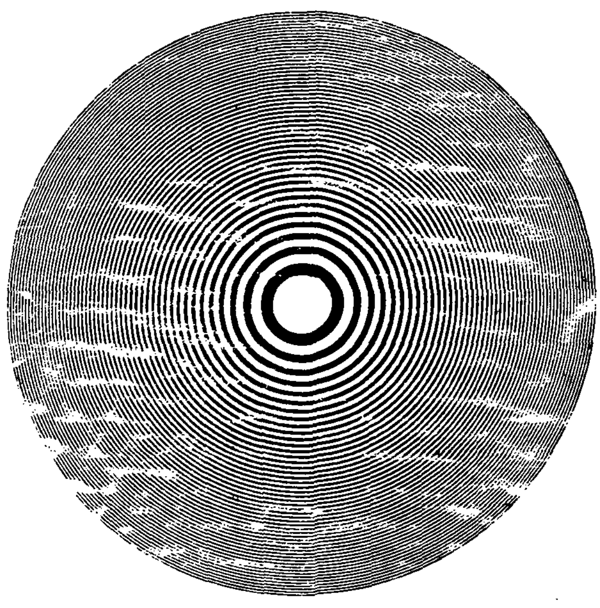

Figure 4. Zone plate.

This zone plate behavior of holograms can be used to explain the imaging properties of more general holograms. The normal target field volume of Figure 1 may be thought of as an aggregate of individual small opaque particles, each of whose specific location (i.e., specific value of Z) is determined by the three-dimensionality of the extended field volume. Radiation diffracted by each

individual particle of the field volume interferes separately and simultaneously with the reference wave to produce an aggregate superposition of many zone-plate-like holograms.

When the interference pattern so produced is developed and reilluminated by the reference wave, the image of each individual particle is simultaneously reconstructed in the same position previously occupied by its respective individual object point. Consequently, any three-dimensionality held by the original field volume is captured by the total reconstructed image.

One of the advantages of the in-line system is its minimum demand on the coherence length of the source used for illumination. The primary disadvantages of the in-line system are its low signal-to-noise figure which is caused by the presence of the transmitted zeroth diffraction order lying coaxial with the image and the fact that, if the particle density becomes too large, the reference beam is attenuated to the point of extinction. If one has a sufficient coherence length source available, one may use an acute-sideband system and negate the primary disadvantages listed above.

Acute-Sideband

This system is basically the regular sideband holographic system. The term acute is derived from the fact that the angle of separation between the reference beam and object beam is intentionally kept as small as possible. Figure 5 displays a possible configuration for such a system. As is seen from the figure, the primary difference is the use of a separate reference beam making some small angle with respect to the object beam. If this angle is kept small, then one retains most of the advantages of the in-line system while overcoming the two distinct disadvantages of the in-line system mentioned above. The primary drawback to this system is that the physical test arrangement may cause the separate reference arm to be sufficiently longer than the object arm that the mismatch will exceed the coherence length of the source employed. Any mismatch in length between the object and reference path length, of course, reduces the useable length of the target field region. A number of things can be done with such a system to overcome this primary disadvantage, for example, folding of the object beam prior to the target field region so as to match the path length of both beams. Further, long coherence length (7 m) ruby laser systems are now available, such that a reasonably large mismatch may be tolerated and still retain sufficient coherence for a useable target field region.

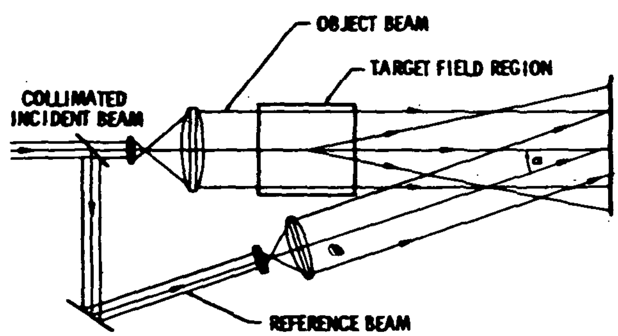

Figure 5. Acute-sideband holography system.

Submicron Particle Detection

Generally speaking, the two above-mentioned systems, which are considered imaging systems, are limited to the detection of particles $\gtrsim$ 10 μm. In order to detect information on particles < 10 μm, one must utilize some scheme for submicron particle detection. Attention is directed to the document by Thompson, 1964. In this article, two separate techniques are fully discussed. The basic principle of one of these techniques, the coherent background technique, is to essentially use the hologram as an

interferogram. Then from the intensity distribution of the diffraction pattern of an individual particle, one determines the radius, r, of the airy disc. This is related to the particle size by

$$2a = \frac{1.22Z\lambda}{r}$$

where 2a is the diameter of the particle and Z is the distance of separation of the particle from the film plane, i.e., object distance. The above equation is, of course, for a particle with circular cross section. However, for a particle with arbitrary cross section, one simply considers 2a to be the largest dimension of the particle. Again, for a complete discussion of these type techniques, attention is directed to the Bibliography.

EXPERIMENTAL RESULTS USING IN-LINE SYSTEM

Chamber Facility and Test Arrangement

The large vacuum chamber utilized to simulate the space environment is shown in Figure 6. The dimension of the inside working volume is 12.2 by 6.1 m. The tests were performed under vacuum conditions with the LN_2 cold walls stabilized at the minimum temperature obtainable. The DT8 panel provided the contamination vent and was positioned in the chamber such that the vent plume was ejected downward. The full angle of the plume, measured in the vicinity of the nozzle plane, was approximately 40 degrees. Because of gravity collimation, the plume may be considered with the vent at approximately 4.6 m from the chamber floor. The typical rate of discharge of the contaminant source was 1.2 to 1.8 lb/min through the nozzle. Some of the runs had air injected into the stream.

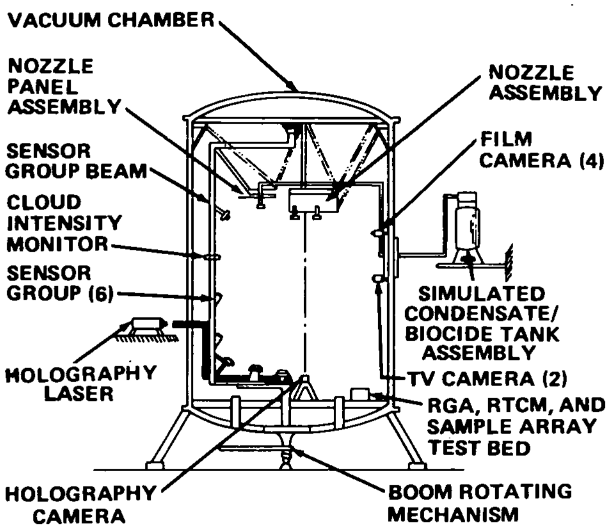

Figure 6. Large vacuum space simulation chamber.

The holography system was mounted in the chamber volume as indicated in Figure 6. The laser beam was enclosed within a 15.3-cm diameter tube to prevent disturbance until the volume to be investigated was illuminated. Active mirrors controlled by hysteresis motors were used to direct the beam through the protective 15.3-cm tubes and to realign whenever it was necessary.

The holographic system was mounted so that the centerline, or optical axis, of the laser beam was as perpendicular as possible to the centerline of the vent plume and at a maximum distance from the orifice of the vent nozzle. Figure 7 shows this position of the laser holographic system as viewed from the top of the vacuum facility. The volume of interest to be recorded holographically is just slightly displaced from the centerline of the vent plume. This sample volume was cylindrically shaped with a cross-sectional area of 7 cm^2 and a length of 50 cm, for a total volume of 350 cm^3 . The intensity of the condensate plume in the region of this sample volume was approximately 32 percent of the total mass flow.

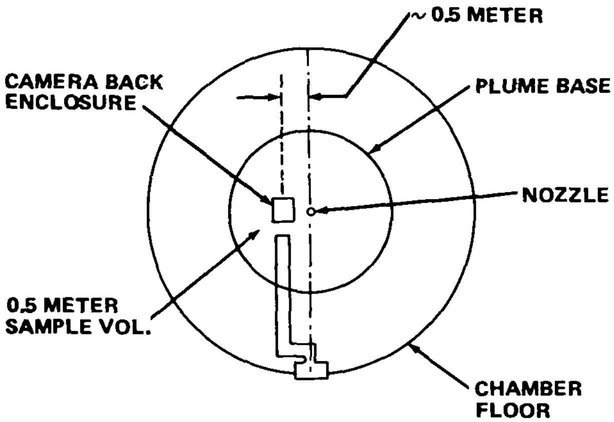

Figure 7. Top view of vacuum system.

Construction System

The holographic system used for the construction or recording of the sample volume was the conventional in-line, Gabor-type system. This technique has the advantage that the particle field can be recorded without disturbing the sample ensemble and the information may be reconstructed for analysis at any later time. Unlike conventional methods which are too slow to satisfactorily sample a dynamic ensemble and which may disturb such an ensemble, this technique is capable of recording the position, size, and velocity of each particle in the field without having the specific depth-of-field problem usually associated with high-resolution photography or microscopy.

While a Gabor-type system was used, one must speak in terms of Fraunhofer holograms because, even though the detector is in the near field of the total ensemble, it is in the far field of the individual particles. Fraunhofer diffraction patterns are formed by the individual particles when the distance from the point source (laser) to the object plane Z' and the distance from the object plane to the recording plane Z is such that

$$Z' >> (\xi^2 + \eta^2)\,\mathrm{max}/\lambda \qquad (8)$$

and

$$Z >> (\xi^2 + \eta^2)\,\mathrm{max}/\lambda \qquad (9)$$

where $(\xi^2 + \eta^2)$ max is the maximum dimension of the diffracting object and λ is the illuminating laser wavelength. By using plane wave illumination, the first restriction can be removed. The second restriction of equation (2) may be relaxed for circular apertures to read

$$Z \geqslant \frac{d^2}{\lambda} \qquad (10)$$

where d is the diameter. For other geometries, d is the magnitude of the greatest dimension. The inequality of equation (3) defines one far field for the particle. Therefore, the recording distance Z may be defined in terms of N far-field distances as

$$Z = N\,\frac{d^2}{\lambda} \quad . \qquad (11)$$

Figure 8 shows a plot of this far-field criterion for particle radii from 1 to 10^{-3} μm and recording distances from 0.01 to 10 m. The horizontal lines indicate the range of the 50-cm volume used in this test. The positive slope diagonal lines represent the range of values of N or the number of far-field distances. Any recording situation lying above this curve will result in images of poor contrast and resolution. The minimum Fraunhofer recording criterion, N=1, is the rightmost diagonal line; any recording situation lying below this line will be in the near field of the particle and will suffer from the two-image problem which plagued Gabor. Since the depth of field is limited by the particle density as well as the recording distance, the negative slope diagonal lines represent the range of particle densities as

they affect the useful sample volume for various size particles. The particle density limits the volume size since all information in the three-dimensional volume must be recorded on a two-dimensional plane. If the magnitude of the particle density is too high, a clean reconstruction is prohibited since the intensity of the undiffracted light (the reference beam) is greatly reduced and, secondly, the information from the farthermost particles does not reach the recording plane.

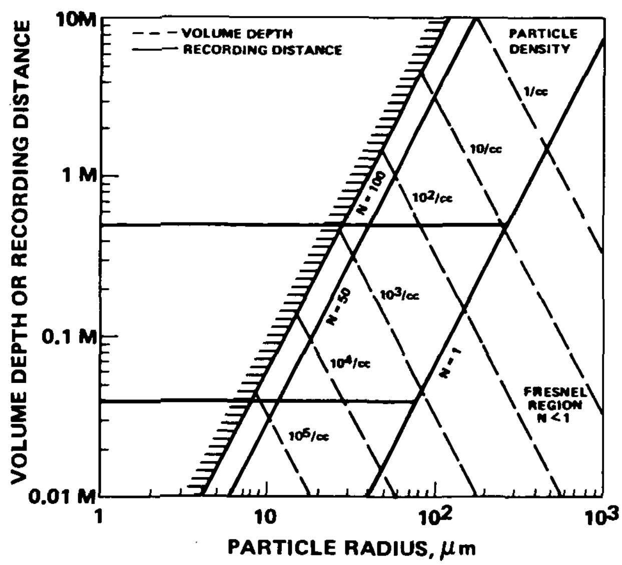

Figure 8. Engineering plot for holography system.

Figure 9 is a diagram of the basic system employed in the present particle analysis tests. For the holographic construction of the sample volume, a 6943-Å ruby laser was used. The output energy is 1 joule per pulse; the coherence length is in excess of 3 m. Radiation from the laser is expanded and collimated and allowed to pass through the sample volume where it is first incident on the photographic film. Radiation passing through the sample volume undiffracted becomes the reference beam; that portion diffracted by the particles of the sample volume constitutes the object beam. The interference between these two beams is recorded at the film plane, and, consequently, the hologram is recorded. The film used was 70-mm film in a Hasselblad back.

After each exposure, the film was mechanically stepped forward to make a new frame available. Exposures were taken throughout the tests at a rate of 2 per minute. The distance Z indicates the extremities of the sample volume with respect to the film plane.

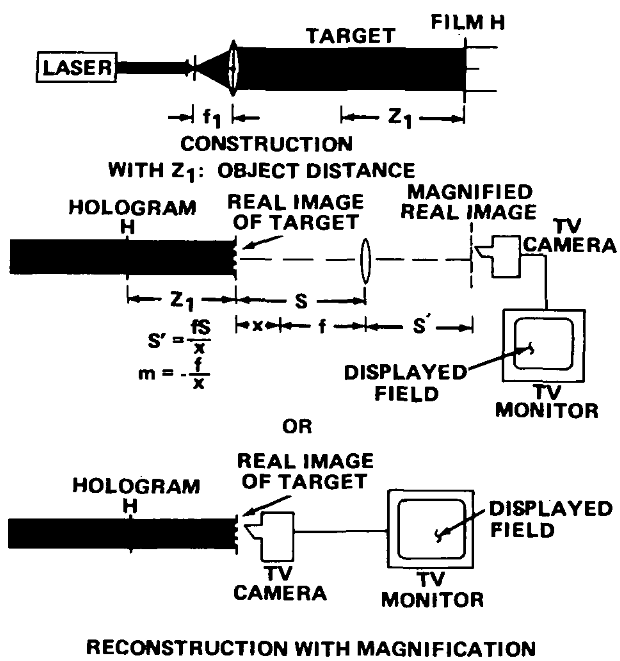

Figure 9. Diagram of holographic system.

Readout System

The reconstruction system utilized is determined by the requirement for system magnification. Two such reconstruction systems are provided in Figure 9. These are essentially the same except for the lens magnification in one and not in the other. Since the present tests utilize the system with the lens, this system will be described first,

after which the use of the second type system will be obvious.

After the hologram is developed and dried, it is placed in the expanded parallel laser beam from a 6328-Å HeNe continuous laser. The real image of the recorded sample volume now appears downstream of the hologram and extends from the hologram a distance Z to the end of the reconstructed sample volume. The image distance Z is essentially the same as the object distance Z except that it is slightly compressed by the ratio of the reconstruction wavelength to the construction wavelength. The optics for the remainder of this system is set to focus on a calibrated square, positioned precisely at the distance Z from the hologram. Therefore, the most extreme plane of the reconstructed sample volume is the plane in focus. Any particles whose images lie in this plane will be the only ones that will appear in focus on the TV monitor. The optics per se needs no explanation; it merely enlarges anything in its object plane and translates the image downstream to the image distance for the system. The total lens magnification used was approximately 3.8; the overall system magnification was 230, including the electronic magnification of the TV unit.

To reconstruct the entire sample volume, one simply uses a micrometer to translate the hologram throughout the entire distance Z. Thus, each plane is sequentially singled out throughout the entire volume. Further, for each separate plane that is sequentially placed a distance S from the lens, all particles in that plane will come into focus on the television unit and, consequently, will be counted and sized. Actually, this translation of the hologram is not precisely a continuous one, but rather a discrete translation of 2000 μm between planes. This is successively performed until the entire volume is searched.

PRELIMINARY RESULTS

A photograph of the laboratory readout system is shown in Figure 10. The system is mounted on a 2-m optical bench with the $\vec{k}$ vector, or propagation vector for the 6328 Å radiation, directed out of the figure toward the TV camera and small monitor. All component holders utilized possess x, y, and z micrometer translators. The large monitor seen in the right of the figure was used for the actual particle sizing. Since the sizing was performed manually, a template with various calibrated sizes was constructed for use in determining the size of the focused particles. The various size particles were recorded in specific ranges in a histogram form. The smallest particle which could be consistently resolved within the volume was 20 μm. It was possible, with this readout system, to resolve 5-μm particles which were standing on the surface of the bandpass filter of the recording holographic system. This filter was located approximately 3 cm from the film plane for the system. Since these particles were found on both sides of the filter, their origin is not precisely known and they were not included in the final particle count.

Figure 11 shows some of these small particles. The black square is a calibrated particle, 35 μm on each side, which is located in and defines the plane of focus for the system. The obvious in-focus particles are the four at the top which form a parallelogram and the inverted dipper shape traced out in the center, among others.

Using a small opaque stop positioned precisely at the focal point of the magnifier lens for the system, one can block all parallel rays passing through this lens and, consequently, increase the signal to noise, for

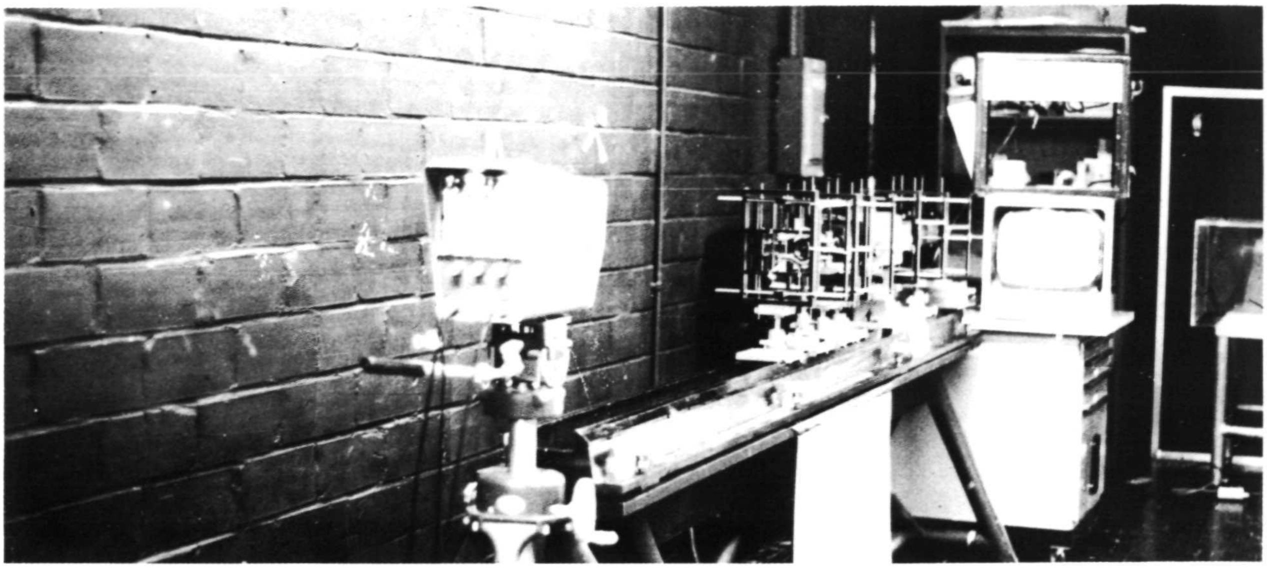

Figure 10. Photograph of laboratory readout system.

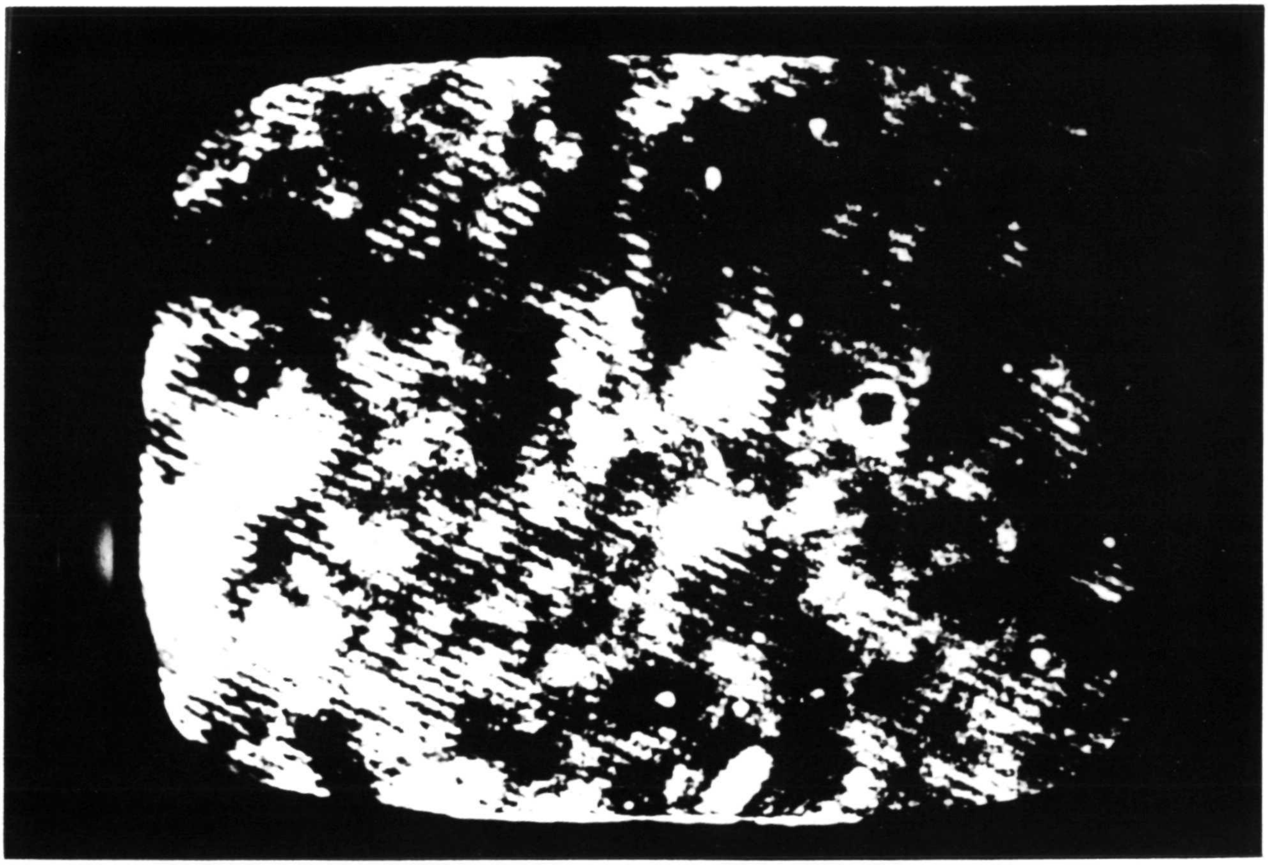

Figure 11. Photograph of reconstructed particles.

this view, by reducing the background caused by out-of-focus particles. Using a 1000-μm opaque stop in such a fashion, Figure 12 shows the improvement obtained over the arrangement in Figure 11 for the same view of particles. The large white area on the right of center is caused by diffraction of the 35-μm square in the plane of focus for the system. The increase in signal to noise is quite apparent. It should, of course, be pointed out that the 1000-μm stop used here was too large and, consequently, stopped useful information as well as background. Further experimentation with a 100-μm opaque stop showed improvement. Also, the presence of the stop tended to obscure the very large particles; perhaps one should move the stop in and out of position while looking for these larger particles.

To demonstrate the effect of increasing the contrast of the camera and/or monitor, attention is directed to Figures 13 and 14. The change is particularly noticeable in the large out-of-focus particles. However, this adjustment must be used judiciously or one begins to alter the size of the in-focus particles.

The effect of a 2-mm translation of the real image along the direction of the propagation vector is demonstrated in Figures 15 and 16. The largest particle found in this hologram is shown in Figure 17. This particle occurred near the end of the volume and appeared to stand alone. It was approximately 300 by 175 μm and caused considerable background as it was approached along the z axis for about 4 to 6 cm. Once it came into focus, the fact that it was standing alone was

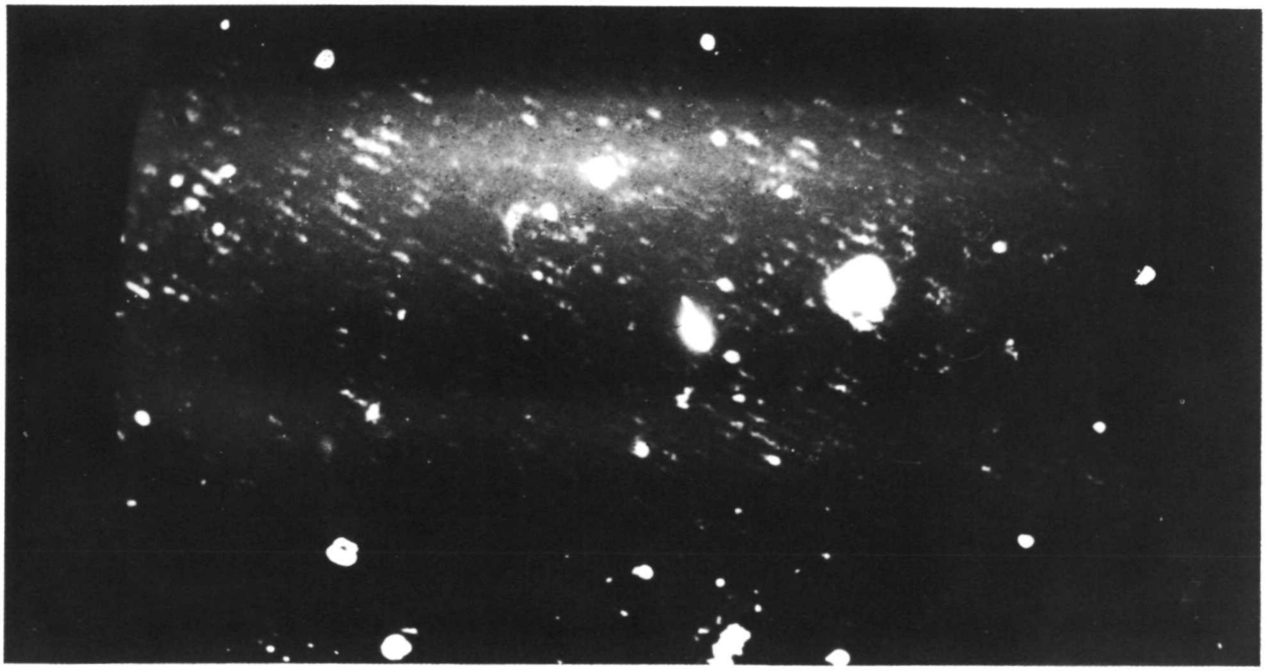

Figure 12. Photograph of reconstructed particles with dc stop.

Figure 13. Photograph of reconstructed particle field.

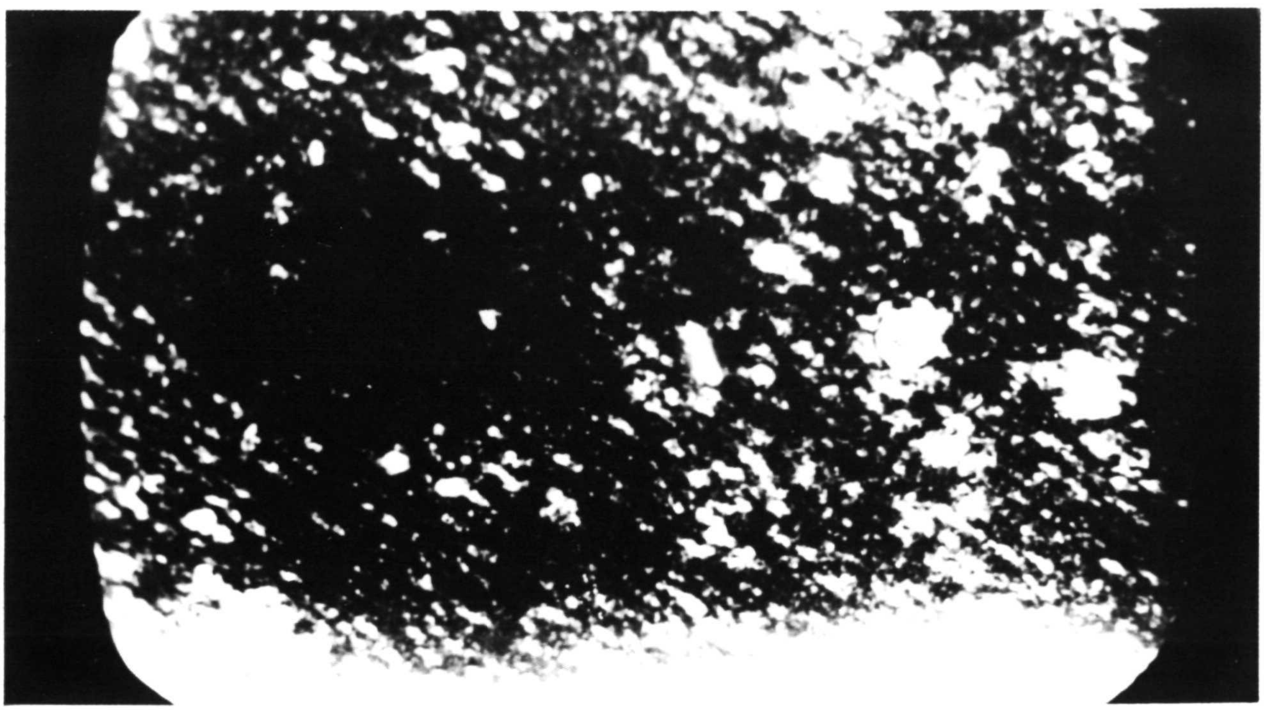

Figure 14. Photograph of reconstructed particle field with increased contrast.

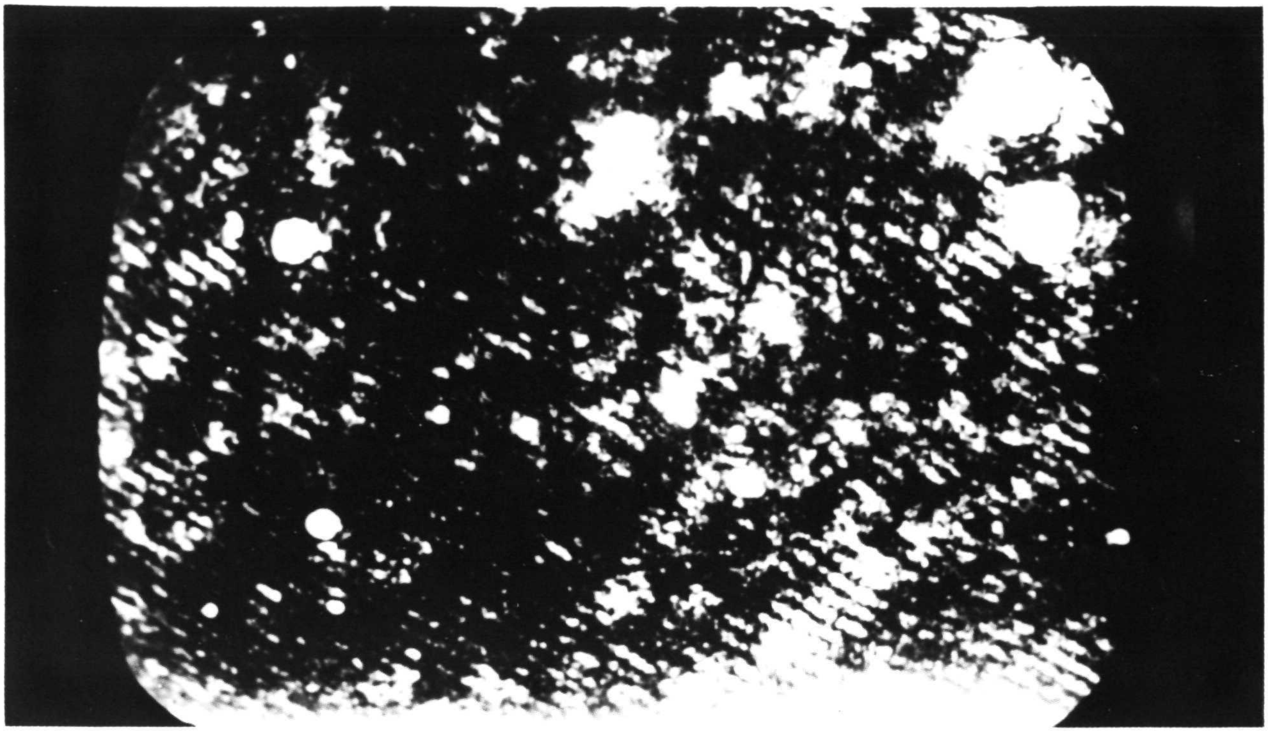

Figure 15. Photograph of particle field at position Xo.

Figure 16. Photograph of particle field at position Xo + 2 mm.

Figure 17. Photograph of largest particle observed.

quite obvious. A 1000-μm translation along the z axis was sufficient to take it in and out of focus. The small black square in the center of the large particle is, once again, the 35-μm calibrated particle in the plane of focus of the system.

Figure 18 is a histogram showing the results of this preliminary data for the particle density. The peak density occurred for the particles having a mean diameter of 30 μm. The density decreased monotonically from that point. No particles larger than approximately 300 μm were found. There may have been particles below 20 μm but, if so, they were below the system resolution for the volume of interest.

The velocity information was obtained from a double-pulsed hologram of the dynamic volume with the pulses separated by 100 μsec. To obtain the particle velocity from such a hologram, one must find the magnitude of the position vector between the two resultant

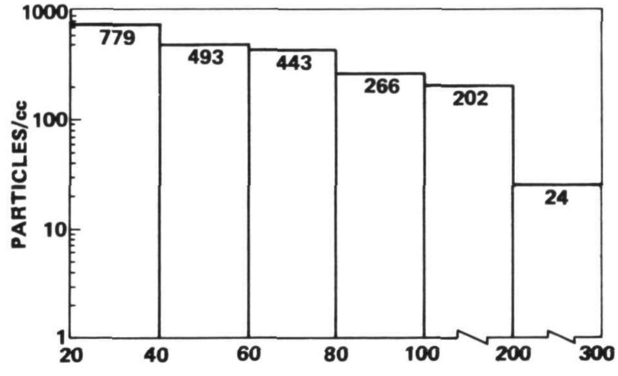

Figure 18. Histogram of particle size distribution.

images of each single particle. The procedure for this is shown in Figure 19. One must first locate the two images of the particle of interest, i.e., a doublet. The first one is placed in focus; this provides a reference position. Then, by measuring the magnitude of the three orthogonal components necessary to place the second image in focus and coincident with the first image, one obtains sufficient information for the calculation of the magnitude of the total position vector R. Consequently, R, along with the known time delay between pulses, provides the magnitude of velocity for that doublet. A velocity of 20 m/sec was found for a single doublet in this test.

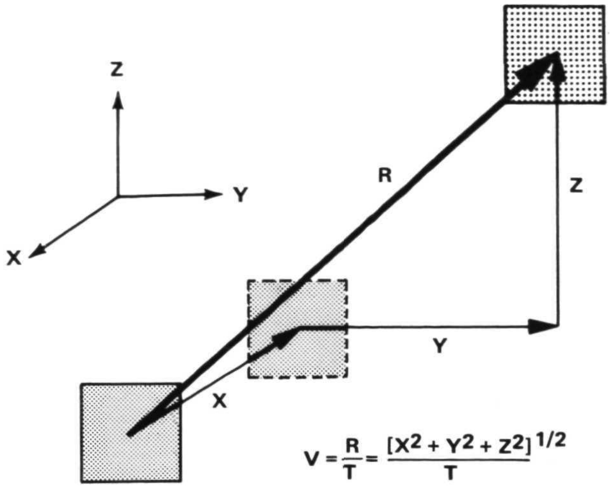

Figure 19. Method for velocity detection of a doublet.

CONCLUSIONS

Although in the experimental use of the in-line holographic system it was possible to obtain the desired particle information, the particle density was too high. There are several things which one may do to increase the signal to noise for the system. An opaque dc stop may be utilized in a dynamic fashion to reduce the background. A dielectric dc stop with some percentage transmission may also be used. Finally, other electronic possibilities are open if the situation warrants it.

In spite of the high particle density and consequent reduction in hologram quality, the holographic technique proves to be a tailor-made detector for this type of particle study. Further, for the three systems described, it was pointed out that the method of detection constitutes an unequivocal nondestructive testing technique which offers extreme promise for quantitative study of particle fields.

George C. Marshall Space Flight Center
National Aeronautics and Space Administration
Marshall Space Flight Center, Alabama, November 1972
964-50-00-000 OMSF

BIBLIOGRAPHY

Belz, R. A.: Analysis of the Techniques for Measuring Particle Size and Distribution from Fraunhofer Diffraction Patterns. AEDC-TR-68-125 (AD674741), Sept. 1968.

____:Characteristics of an In-Line Hologram Image. Proc. of Electro Optical System Design Conference, Sept. 1971.

Born, M. and Wolf, E.: Principles of Optics, 3rd Ed., Pergamon Press, New York, 1967.

Clayton, R. M. and Wuerker, R. F.: Applying Holography to Reacting Spray Studies, Holography Instrumentation Applications. NASA SP-248, Jan. 1970.

DeVelis, J. B.; Parrent, G. B.; and Thompson, B. J.: Image Reconstruction with Fraunhofer Holograms. J. Opt. Soc. Am., vol. 56, Apr. 1966, pp. 423-427.

DeVelis, J. B. and Reynolds, G. O.: Theory and Applications of Holography. Addison-Wesley Publishing Co., Reading, Mass., 1967.

Farmer, W. M.: Dynamic Holography of Small Particle Fields Using a Q-Spoiled Laser. Master's Thesis, The University of Tennessee, Knoxville, 1968.

Fourney, M. E.; Matkin, J. H.; and Waggoner, A. P.: Aerosol Size and Velocity Determination via Holography. Rev. Sci. Instr., vol. 40, Feb. 1969, pp. 205-213.

Gabor, D.: Microscopy by Reconstructed Wavefronts. Proc. Roy. Soc., vol. A197, Mar. 1949, pp. 454-487.

Glasstone, S.: Textbook of Physical Chemistry. D. Van Nostrand Company, Princeton, N. J., 1959.

Goodman, J. W.: Introduction to Fourier Optics. McGraw-Hill Book Co., N.Y., 1968.

Heggins, G. C.: Methods for Engineering Photographic Systems. Appl. Opt., vol. 3, Jan. 1964, pp. 1-10.

Kodak Plates and Film for Science and Industry. Kodak Publication No. p-9, Eastman Kodak Company, N.Y., 1967.

Parrent, G. B. and Thompson, B. J.: On the Fraunhofer (Far-Field) Diffraction Patterns of Opaque and Transparent Objects with Coherent Background. Optics Acta, vol. 11, Jul. 1964, pp. 183-194.

Reynolds, B. O. and DeVelis, J. B.: Hologram Coherence Effects. IEEE Trans. on Antennas and Propagation, AP-15, Jan. 1967, pp. 41-48.

Shofner, F. M., et al.: Fundamentals of Holographic Velocimetry. Proceedings, 1969 International Congress on Instrumentation in Aerospace Simulation Facilities, May 1969.

____:Processing Holographic Velocimetry Data. Proceedings, 1969 International Congress on Instrumentation in Aerospace Simulation Facilities, May 1969.

Silver, S.: Microwave Antenna Theory and Design. M.I.T. Radiation Laboratory Series, No. 12, Boston Technical Publishers, Boston, Mass., 1967.

Silverman, Bernard A.: A Laser Fog Disdrometer. J. Appl. Metrology, vol. 3, Dec. 1964, p. 792.

Stroke, G. W.: An Introduction to Coherent Optics and Holography. Academic Press, N.Y., 1966.

BIBLIOGRAPHY (Concluded)

____:An Introduction to Coherent Optics and Holography. 2nd Ed., Academic Press, N.Y., 1969.

Thompson, B. J.: Diffraction by Opaque and Transparent Particles. Society of Photo-Optical Instrumentation Engineers Journal, vol. 2, December 1963-January 1964, pp. 43-46.

____:A New Method of Measuring Particle Size by Diffraction Techniques. Japanese Journal of Applied Physics, vol. 4, Supplement I, 1965, pp. 302-307.

Thompson, B. J. and Ward, J. H.: Particle Sizing–The First Direct Use of Holography. Scientific Research, vol. 1, Oct. 1966, pp. 37-40.

Thompson, B. J.; Parrent, G. B.; Ward, J. H.; and Justh, B.: A Readout Technique for the Laser Fog Disdrometer. J. Appl. Metrology, vol. 5, Jun. 1966, pp. 343-348.

Thompson, B. J.; Ward; J. H.; and Zinky, W. R.: Application of Hologram Techniques for Particles Size Analysis. Appl. Opt., vol. 6, Mar. 1967, pp. 519-526.

Trolinger, J. D.; Belz, R. A.; and Farmer, W. M.: Applications of Holography in Environmental Science. Paper presented at the 15th Annual Technical Meeting of the Institute of Environmental Sciences, Anaheim, California, Apr. 1969.

____:Holographic Techniques for the Study of Dynamic Particle Fields. Appl. Opt., vol. 8, May 1969, pp. 957-961.

Ward, J.: Laser Fog Disdrometer System. Air Force Cambridge Research Laboratories Report No. AD656-487, Bedford, Mass., Jun. 1967.

Zinky, W. R.: Hologram Camera and Reconstruction System for Assessment of Explosively Generated Aerosols. U.S. Army Edgewood Arsenal TO-B-65-90, Chemical Research and Development Laboratories, Edgewood Arsenal, Md., Oct. 1965.

NASA-Langley, 1973 —— 14

"The aeronautical and space activities of the United States shall be conducted so as to contribute . . . to the expansion of human knowledge of phenomena in the atmosphere and space. The Administration shall provide for the widest practicable and appropriate dissemination of information concerning its activities and the results thereof."

—NATIONAL AERONAUTICS AND SPACE ACT OF 1958

NASA SCIENTIFIC AND TECHNICAL PUBLICATIONS

TECHNICAL REPORTS: Scientific and technical information considered important, complete, and a lasting contribution to existing knowledge.

TECHNICAL NOTES: Information less broad in scope but nevertheless of importance as a contribution to existing knowledge.

TECHNICAL MEMORANDUMS: Information receiving limited distribution because of preliminary data, security classification, or other reasons. Also includes conference proceedings with either limited or unlimited distribution.

CONTRACTOR REPORTS: Scientific and technical information generated under a NASA contract or grant and considered an important contribution to existing knowledge.

TECHNICAL TRANSLATIONS: Information published in a foreign language considered to merit NASA distribution in English.

SPECIAL PUBLICATIONS: Information derived from or of value to NASA activities. Publications include final reports of major projects, monographs, data compilations, handbooks, sourcebooks, and special bibliographies.

TECHNOLOGY UTILIZATION PUBLICATIONS: Information on technology used by NASA that may be of particular interest in commercial and other non-aerospace applications. Publications include Tech Briefs, Technology Utilization Reports and Technology Surveys.

Details on the availability of these publications may be obtained from:

SCIENTIFIC AND TECHNICAL INFORMATION OFFICE

NATIONAL AERONAUTICS AND SPACE ADMINISTRATION

Washington, D.C. 20546